View metadata, citation and similar papers at core.ac.uk
brought to you by CORE
provided by University of Brighton Research Portal

EFFECT OF EXTREME WETTING SCENARIOS ON POOL BOILING

T. Valente[1], tomas.valente@tecnico.ulisboa.pt
I. Malavasi[2], ilenana.malavasi@gmail.com
E. Teodori[1], e.teodori@dem.ist.utl.pt
A.S. Moita[1]*, anamoita@dem.ist.utl.pt
M. Marengo[2,3], m.marengo@brighton.ac.uk
A.L.N. Moreira[1], moreira@dem.ist.utl.pt

[1]IN+ - Instituto Superior Técnico, Universidade de Lisboa, Av. Rovisco Pais, 1049-001 Lisbon, Portugal
[2]Dept. of Eng. and Applied Sciences, University of Bergamo, Viale Marconi 5, 24044 Dalmine, Italy
[3]University of Brighton, School of Computing, Engineering and Mathematics, Lewes Road, BN2 4GJ Brighton, UK

ABSTRACT

This study focuses on the detailed description of the heat transfer and bubble dynamics processes occurring for the boiling of water over surfaces with extreme wetting regimes, namely hydrophilicity and superhydrophobicity. The wettability is changed at the expense of modifying the surface chemistry and without strong variations in the mean surface roughness. Furthermore, a detailed analysis is presented, showing the temporal evolution of the bubble growth diameter together with bubble dynamics, which may serve for future comparison with numerical simulations.

The results show a particular trend of the boiling curve obtained for the superhydrophobic surfaces, as the heat flux increases almost linearly with the superheat, until reaching a maximum value after which it does not further increase. This occurs because a large bubble is formed over the entire surface just at 1ºC superheat, as a result of the almost immediate coalescence of the bubbles formed at the surface. This behaviour is in agreement with the so-called "quasi-Leidenfrost" regime recently reported in the literature.

Regarding bubble dynamics, the results suggest that the existing models can predict the trend of the bubble growth using the micro-contact angle (complementary to bubble contact angle) for the hydrophilic surfaces, but cannot accurately predict bubble size, as they do not account for interaction mechanisms. Also they cannot describe the particular bubble growth phenomenon observed for the superhydrophobic surfaces. Quasi-static angles cannot provide any satisfactory results when used in the models to predict the bubble growth diameter, although they follow an evolution similar to that of the micro-contact angle and are supplemental to the bubble contact angle. In line with this, trends can be observed between the average bubble departure diameter and bubble departure frequency with both the bubble and the quasi-static advancing angle. These results suggest that the parameter which can accurately relate the bubble growth with the surface wettability is the bubble contact angle (or from the wall side, the so-called micro-contact angle), but apparent angles follow supplemental evolution, being therefore useful to identify qualitative trends.

KEYWORDS
Pool Boiling, Two-phase systems, Wettability, Boiling onset, Boiling Curve

INTRODUCTION

Enhancement of pool boiling heat transfer is often achieved by altering surface properties. The evolution observed in micro and nano fabrication techniques within the last decade provides the researchers the opportunity to test a wide range of surface treatments, which quickly evolved from the micro-patterned surfaces with structures of the order of hundreds of microns, as obtained for instance by Courty and Foust (1955) to nanocoatings (e.g. Takata, et al., 2006, Phan et al., 2009). However, many of these treatments simultaneously alter surface topography and wettability in a non-systematic way, turning difficult to understand dominant effects on the boiling mechanisms, which lead to the actual enhancement on the heat flux that is often reported in these studies. In fact the wettability is affected by the chemistry of the surface (and of the working fluid) and by the surface topography. However, it is possible and desirable to separate them at some extent, as recently shown by Bourdon et al. (2012, 2013). The surface wettability is usually roughly quantified by the apparent contact angle θ_{app}, which is obtained at the thermodynamic equilibrium between the interfacial tensions acting at liquid-solid-vapor contact interfaces (often measured on a sessile drop deposited on the surface). Based on this apparent angle, it is widely accepted that a surface is lyophilic (i.e. promotes the liquid spreading) for $0< \theta_{app}<90^o$ and lyophobic (i.e. repels the liquid) for $\theta_{app} >90^o$. The terms hydrophilic/hydrophobic, which are commonly used for liquid attractive/repellent surfaces, derive from the specific attraction/repellency of water. The boundaries for extreme wetting scenarios, namely superhydrophilicity and superhydrophobicity are still debated in the most recent literature, as universal criteria to determine stable extreme wetting regimes are not easily defined. It is known that the heterogeneous wetting regime associated to superhydrophobicity may not be stable and may not hold, as an activation energy barrier is transposed, and the contact line slowly moves (e.g. He et al., 2003). Hence, the most representative measures are given by the quasi-static advance or receding (apparent) contact angles and by the hysteresis, which is basically the difference between the advancing and the receding angles. So, based on this, several authors, such as Bushan et al. (2008) consider that a surface is superhydrophobic for $\theta_{rec} >135^o$, as long as the hysteresis is lower than 10^o. These advancing and receding angles are also argued to be more representative of dynamic processes, which has been demonstrated for drop impacts (for example Antonini et al., 2012), but may be important also for bubble dynamics (e.g. Mukherjee and Kandlikar, 2007).

The various experiments performed on pool boiling over superhydrophobic surfaces vs hydrophilic surfaces (e.g. Takata et al., 2009, 2012, Phan et al., 2009, Betz et al., 2013) are consistent in the description of the main trends observed: bubble nucleation starts at lower superheat values on a superhydrophobic surface, as the energy barrier necessary for nucleus generation is smaller. However, despite nucleation is favoured, rewetting is not, so the superhydrophobic surface inhibits bubble release. On the contrary, a superhydrophilic surface requires larger superheat to start bubble nucleation, but find it easier to release the vapour bubble. As a result, the onset of boiling starts at very low superheat values on superhydrophobic surfaces, but then the force balance does not favour the bubble release form the surface, so large bubbles stay for longer attached on the surface and coalesce, leading to a Critical Heat Flux condition at low superheat values. The opposite trend is observed for the boiling curves for hydrophilic surfaces. Based on these observations, several authors promptly passed on to an "optimum" surface, considering an adequate superhydrophilic/superphydrophobic patterning of the surface. However, the basic governing mechanisms occurring at these extreme wetting regimes are far to be understood. Detailed description of the nucleation process and of bubble dynamics such as those performed for instance by Phan et al. (2009), McHale and Garimella (2010) and Moita et al. (2015) are still scarce and do not allow establishing the accurate relation between bubble dynamics and the aforementioned trends of the boiling curves. Also, the basic nucleation mechanisms were never properly related to the wettability as it is still unclear which is the accurate quantity to use. Hence, several authors consider a rough approximation of the apparent angle to be representative of the contact angle at bubble growth in the expressions to predict the bubble departure diameter, such for example the Fritz equation (Fritz, 1935). The accuracy of Fritz equation has been debated several times, particularly when dealing with hydrophobic and superhydrophobic surfaces (e.g. Matkovic and Koncar, 2012) and Phan et al. (2009) even report an opposite trend of the bubble growth with the contact angle, when compared to that given by the Fritz equation. These authors proposed instead that the micro-angle defined during bubble growth is more appropriate to estimate the bubble diameter, including it on the so-called energy factor, which basically accounts for the ratio between the volume of a sphere which has a micro-contact angle and the surface of the full sphere with the same diameter. Phan et al. (2009) further show that this angle is actually very small at nucleation and then increases during bubble growth for hydrophilic surfaces, occurring the opposite for hydrophobic surfaces. Then, based on geometrical argument the authors show that the energy required to activate the nucleation site and initiate the following bubble generation is actually larger for a lower micro-contact angle. However, when building up the whole model, Phan et al. (2010) argue similarity between the micro and the apparent contact angles at bubble departure, for particular conditions. Finally it is important also to notice that in presence of a flow, the drag may contribute to either the drop detach from the wall or the formation of a vapour film, depending on the flow velocity near the wall and the thermal boundary layer. In the first case the result is an

improvement of the boiling efficiency, i.e. the lower superheat is associated with higher heat transfer coefficients in case of hydrophobic surfaces (Rioboo et al., 2009).

In this context, the present work aims at contributing with additional information to allow a more adequate description of bubble dynamics and discusses which are the most adequate parameters relating these dynamic processes with surface wettability. Hence, boiling curves obtained for extreme wetting scenarios (hydrophilic vs superhydrophobic) are discussed in detail, together with the temporal evolution of several quantities used to describe bubble dynamics, namely bubble diameter, bubble emission frequency and bubble contact angle. The surface topography is varied within these extreme wetting conditions, in a systematic and controlled way to assess on its role in a situation for which the wettability is mainly controlled by the chemical modification of the surface. The quantification of these variables is supporting further numerical simulations of the boiling process.

EXPERIMENTAL ANALYSIS

Experimental set-up

The set-up is mainly composed by a boiling chamber, where the experiments are performed, a degassing system in which the fluid is degassed, pressurized and constantly heated and a filling and evacuating circuit that connects the boiling chamber respectively to the degassing station and to the waste fluid container, being the later at ambient pressure. The pressure and the temperature inside the boiling chamber are accurately controlled (the temperature is controlled with a precision of 1ºC and for the pressure control the precision is 5mbar). The entire heating block of the pool boiling test section is isolated with Teflon, from the outside and the pool boiling chamber is isolated with rubber. Heaters disposed inside and on the outer surfaces of the boiling chamber are controlled by a PID controller to assure that the liquid remains inside the chamber at saturation temperature. The pressure is controlled by means of two electronic valves that respond to the measures given by a pressure transducer (OMEGA DYNE Inc) inside the pool, using a home-made software based loop control. This control system reacts to pressure variations in the order of 5mbar. The refilling and the entire measurement processes are automatically controlled by this software. The temperatures are sampled using type K thermocouples. The signal is acquired and amplified by a National Instruments DAQ board plus a BNC2120. The acquisition frequency is 100Hz. The heating block, which heats and accommodates the different surfaces, is formed by a copper cylinder inside which a cartridge heater (up to 315W) is placed. As aforementioned, also the cylinder is isolated with Teflon. The surfaces are positioned into the heating block using a custom made system with bolts and springs, to assure the perfect thermal contact. The bolts contacting the surface are made from PEEK (polyether ether ketone) to minimize heat transfer effects from the surface to the bolts. The heat flux is measured using a thin heat flux meter (Captec Entreprise ®) custom made to fit perfectly to the heating block. This heat flux meter, which is placed between the copper cylinder and the surface has a sensitivity of 2.21mV/(W/m^2).

Methodology and diagnostic techniques

The test surfaces are characterized in terms of their superficial topography and wettability, as detailed in the following paragraphs. The quasi-static advancing and receding angles are evaluated, together with the hysteresis, before and after each test (corresponding to a single boiling curve) for each surface used. Surface topography is also checked. This procedure ensures the exact definition of the boundary conditions related to the wettability and allows inferring the effect of surface ageing on the wettability and, consequently on the pool boiling curves. Then, pool boiling curves are constructed for each test surface, which are obtained by slowly imposing the heat flux in small increasing power steps. For each power step increased, bubble dynamics and nucleation mechanisms are also characterized based on high-speed visualization, using a high-speed camera (Phantom v4.2 from Vision Research Inc., with 512x512pixels@2200fps). Quantitative information regarding bubble dynamics is further obtained by image post-processing procedures.

The working fluid used is degassed distilled water. The thermo-physical properties relevant to this study are summarized in Table 1.

Table 1 Thermophysical properties of the liquids used in the present study, taken at saturation, at 1.013×10^5Pa.

Property	Water
T_{sat} (°C)	100
ρ_l (kg/m^3)	957.8
ρ_v (kg/m^3)	0.5956
μ_l (mN m/s^2)	0.279
c_{pl} (J/kgK)	4217
k_l (W/mK)	0.68
h_{fg} (kJ/kg)	2257
σ (N/m)x10^3	58

Surface preparation. Stainless steel surfaces are prepared to have dissimilar topographic and wetting properties. The numerous surfaces used in this study (nearly 40) are categorized in 4 main groups: RAW – "smooth" hydrophilic surfaces, ROUGH – "rough" hydrophilic surfaces, RAW SHS and ROUGH SHS, representing superhydrophobic surfaces with identical roughness amplitude as that of the hydrophilic ones. The superhydrophobic surfaces are obtained at the expense of a chemical coating (a commercial compound called Glaco Mirror Coat Zero, from Soft99 Co, which is mainly a perfluoroalkyltrichlorosilane combined with perfluoropolyether carboxylic acid and a fluorinated solvent). All the surfaces are first cleaned, following the main steps: a) 30 min in an ultrasonic bath in water at 40ºC, b) drying with compressed air and c) 30 min in an ultrasonic bath in acetone at 40ºC. Then the coating is applied as in Malavasi et al. (2015). The aforementioned cleaning procedure must be repeated for each surface and for all the boiling curves.

Characterization of the surfaces. The homogeneity of surface topography and morphology is checked by Laser Scanning Confocal Microscopy (Leica SP8 Confocal Microscope) using the reflection mode. Then, the stochastic roughness profiles are measured using a Dektak 3 profile meter (Veeco) with a vertical resolution of 200Angstroms. These profiles are further processed to obtain the mean roughness (determined according to standard BS1134) and the mean peak-to-valley roughness (determined following standard DIN4768). Average representative values of R_a and R_z are taken from 10 measurements distributed along the entire surface.

Wettability is quantified by the apparent quasi-static advancing and receding angles. Hystersis is also evaluated for the coated surfaces to assure that it was lower than 10º (following the criterion presented in the Introduction). The measurements are performed at room temperature (20ºC), using an optical tensiometer (TETA from Attension). The angles are evaluated from the images taken within the tensiometer, using a camera adapted to a microscope. The images (with resolution of 15.6 μm/pixel, for the optical configuration used) are post-processed by a drop detection algorithm based on Young-Laplace equation (One Attension software). The accuracy of these algorithms is argued to be of the order of ± 0.1º (Cheng, 1990). A more realistic value of ±1º is considered as contact angle measurement accuracy. The precision is limited by the repeatability and the homogeneity of the surface treatments.

Table 2 depicts the main characteristics of the four categories of surfaces defined for the present study. The contact angles were quite reproducible. The values presented here are taken as an average of 3 representative measurements distributed along the surface. Deviations in R_a were admitted around 10% within each category.

Table 2 Main topographical and wetting characteristics defined for the four categories of surfaces used in the present study.

Category	Surface material	R_a [μm]	R_z [μm]	θ_{adv} [º]	θ_{rec} [º]	Hysteresis $\Delta\theta$ [º]
RAW	Stainless steel	0.06	0.09	85.3	<20	>10
ROUGH	Stainless steel	1.20	1.58	90.75	<20	>10
RAW SHS	Stainless steel coated with Glaco	0.06	0.09	166	164	2
ROUGH SHS	Stainless steel coated with Glaco	1.20	1.58	166	164	2

Pool boiling curves. The boiling curves are obtained under imposed heat flux conditions on the surface, with continuous control and monitoring of the surface temperature, liquid temperature and pressure inside the pool boiling chamber. The curves were obtained at ambient pressure (1bar±5mb) for each surface by varying the

imposed heat flux in steps. Each curve is averaged from 5 experiments. The main uncertainties of the quantities related to temperature measurements are ±1.2% and are assessed following the procedures recommended in Abernethy et al. (1985). Detailed description of the measurement procedures and determination of error sources can be found in Moita et al. (2015).

Image post-processing for the characterization of the nucleation mechanisms and bubble dynamics. The characterization of the nucleation mechanisms and bubble dynamics is based on the measurement of several quantities obtained from high-speed visualization and image post-processing. The images are recorded with a frame rate of 2200fps. For the optical configuration used here, the spatial resolution is 9.346μm/pixel. A home made code developed in MATLAB enables determining the temporal evolution of the bubble diameter (until detachment), bubble contact angle, velocity of the bubble centroid, velocity of the contact line and bubble departure frequency. The temporal evolution of bubble growth is measured for each test condition, from the entire bubble growth period until detachment. Then, averaged values are taken, for the instant of bubble detachment for various bubble detachment events. The bubble departure frequency is estimated by counting the number of events for a defined time interval. The measurement uncertainties, determined as in Moita et al. (2015) are evaluated to be always lower than 0.7% for the departure diameter and velocity of the bubbles' centroid.

RESULTS AND DISCUSSION

Figure 1 depicts the boiling curves obtained for the hydrophilic and superhydrophobic surfaces with the lowest roughness amplitudes. The curves show significantly different trends, which are qualitatively in agreement with the results reported in the literature (e.g. Takata et al., 2009, 2012, Phan et al., 2009, Betz et al., 2013) and with quite good agreement with the results recently reported by Malavasi et al. (2015), whose experimental conditions are very close to those considered in the present work, except for the highest heat fluxes considered here. Hence, the onset of boiling for the hydrophilic surface occurs approximately for a superheating of 12ºC, followed by the typical increase in the curve slope, associated to the triggering of the nucleate boiling regime. On the other hand, the boiling curve obtained for the superhydrophobic surface has a quite atypical trend. The onset of boiling occurs usually during the first power step, just at 1ºC superheat. The heat flux increases then almost linearly with surface superheating, until reaching a constant value up to which it does not further increase.

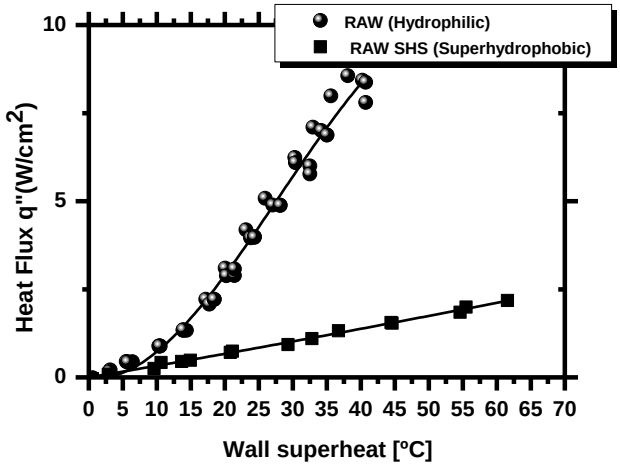

Figure 1. Boiling curves obtained for water over a hydrophilic and a superhydrophobic stainless steel surfaces.

The surface topography clearly plays a secondary role in this case, as the mild increase of the surface roughness does not introduce significant changes in the boiling curves, either in the hydroplhilic or in the hydrophobic surfaces, as shown in Figure 2. In fact, a mild increase of the mean roughness is not likely to introduce a significant modification in the wettability, at least in a monotonic and quantifiable way, which can be related to the apparent angles (e.g. Valente et al., 2015). Also, it is difficult to relate the boiling mechanisms with the average parameters that must be used to characterize surfaces with stochastic profiles (e.g. McHale and Garimella, 2010). Given that, within the range of roughness amplitude considered here, the increase of the mean roughness does not significantly change the apparent contact angles, it is more likely that the roughness will mostly affect the pool boiling heat transfer by promoting the potential increase of the number of active nucleation sites. However, to successfully achieve this goal, one needs to take into account numerous factors such as bubble

and nucleation sites interaction, so that a more systematic approach should be considered, in which the surface topography is altered within a wider range of geometrical parameters, particularly regarding the distance between the potential active nucleation sites (e.g. Teodori et al., 2013).

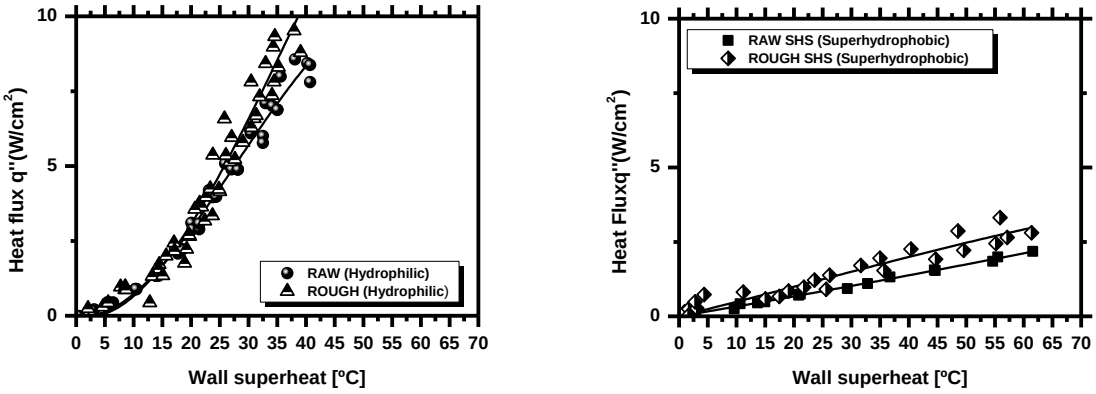

a) **b)**

Figure 2. Effect of surface topography (quantified by the increase of the mean surface roughness) in the boiling curves, for extreme wetting scenarios: a) hydrophilic surfaces, b) superhydrophobic surfaces.

At this point of the discussion, it is worth mentioning that the curves represented here are limited to the low heat flux values, which can be reached with the superhydrophobic surfaces. In fact, further rising the imposed heat flux leads to the disruption of the superhydrophobic coating, which completely modifies the trend of the boiling curve, generating a "biphilic like" behaviour, i.e. resembling the behaviour of a hydrophilic surface with superhydrophobic spots, as reported for instance by Betz et al. (2013). This trend is illustrated in Figure 3.

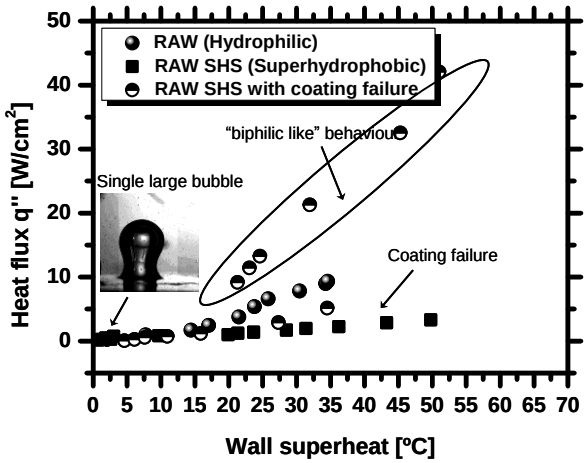

Figure 3. Boiling curve showing a "biphilic like" behaviour, resulting from the disruption of the superhydrophobic coating. The curves obtained for hydrophilic and hydrophobic surfaces are gathered for qualitative comparison.

This occurs at heat flux values much lower than the Critical Heat Flux expected for the hydrophilic surface, so the curves represented here are quite below this critical value.

These results support the argument that hydrophilic surfaces with superhydrophobic spots may provide the best compromise in optimizing pool boiling heat transfer. However, deeper research is required in this topic, to optimize the patterns, which must be supported by an accurate description of bubble dynamics and resultant flow dynamics, which seem to strongly affect pool boiling heat transfer. In these particular conditions, the "biphilic like" behaviour results from a stochastic process, which cannot be controlled and therefore will not be further discussed. The description of bubble dynamics is useful to understand the particular trends of the boiling curves, namely those obtained with the superhydrophobic surfaces. In fact, contrarily to the behaviour reported for instance by Phan et al. (2009) in which, the boiling over the hydrophobic surfaces is similar to that of the hydrophilic in the sense that one can observe several bubbles departing from numerous nucleation sites, so the main difference is observed in the shape, contact angle and size of the bubbles (which are larger for the hydrophobic surface), in the present study, the system is at a metastable equilibrium and just one degree of superheating is enough to activate the numerous nucleation sites. The stochastic profile of the surface promotes

the almost immediate coalescence of the bubbles so that a film vapour is almost immediately formed at 1ºC of superheating. Hence, a large bubble is formed over the entire surface, as illustrated in Figure 3. This behaviour is in agreement with the so-called "quasi-Leidenfrost" regime, reported by Malavasi et al. (2015).

Considering this particular bubble dynamics behaviour, it is worth to perform a more detailed analysis of the bubble growth and detachment mechanisms for these superhydrophobic surfaces, compared with that of the hydrophilic. Figures 4 and 5 depict the temporal evolution of the bubble growth (one bubble) on the superhydrophobic surface compared to that of the hydrophilic one. It is worth noting that, as expected, the waiting time for bubble detachment on the superhydrophobic surface is much larger than that on the hydrophilic, so that the temporal evolution of the bubble growth represented for the superhydrophobic surface corresponds to a single bubble, during the time that nearly 10 bubbles grow and detach from the hydrophilic surface. Hence, while the bubble diameter slowly grows on the superhydrophobic surface over more than 300ms, attaining values larger than 10mm, the bubbles over the hydrophilic surface grow up to 2-2.5mm, within around 10-16ms. The abrupt decrease of the diameter corresponds to the bubble detachment instant, which is not entirely well captured by the post-processing routine. The corresponding bubble departure instant for the superhydrophobic surface could not be captured in this data set, as the waiting period is too long.

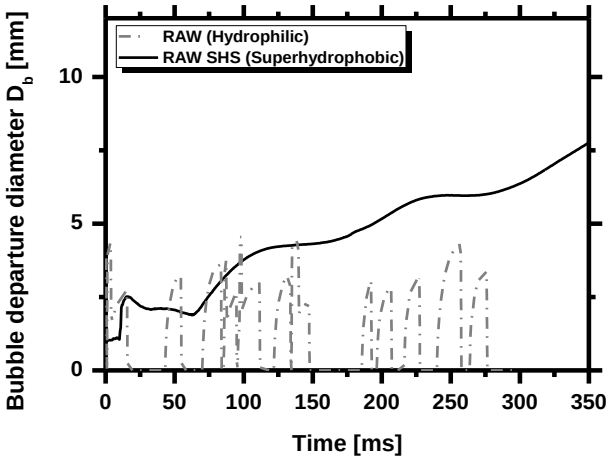

Figure 4. Comparison between the bubble growth on a hydrophilic and a superhydrophobic surfaces.

Regarding the temporal evolution of the contact angle of the bubble, the bubble contact angle starts at a low value and then increases, during bubble growth, until the departure diameter value is reached and then further decreases until bubble detachment. Actually, the bubble contact angle starts with very low values (less than 50º), which are not represented here, as the bubble at this period is yet too small to be accurately tracked and measured by the post-processing routine. The micro-contact angle on the side of the surface (supplementary to the bubble contact angle) has the opposite evolution. This is qualitatively in agreement with the process reported by Phan et al. (2009). On the other hand, given that for the superhydrophobic surface, the large bubble is formed already over a thin vapour film, the bubble already appears with a shape that is indeed very close to that reported by Phan et al. (2009) for hydrophobic surfaces, but the contact angle remains practically constant during the entire slow growing process of the bubble, until it suddenly detaches from the surface.

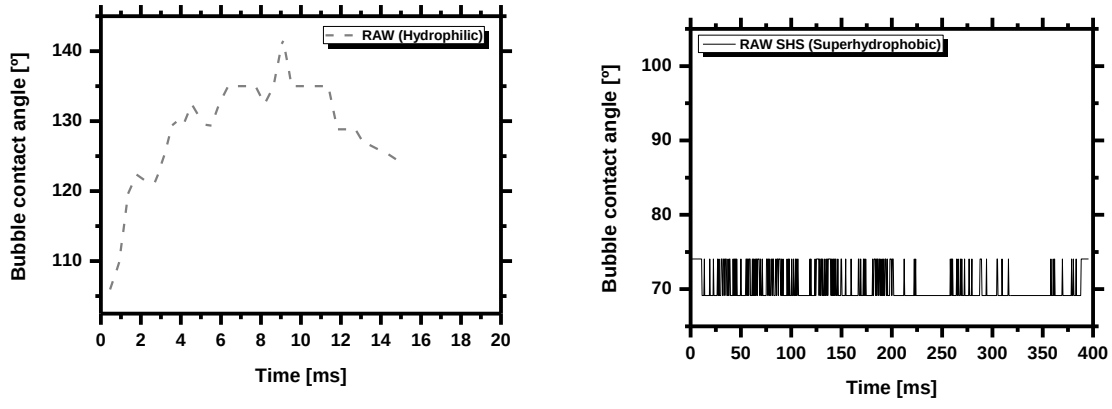

a) **b)**

Figure 5. Temporal evolution of the bubble contact angle during the growth and detachment of a single bubble on: a) a hydrophilic surface, b) a superhydrophobic surface.

These bubble growing processes are schematically illustrated in Figure 6. The images shown in Figure 6 are mainly the post-processing of the real images taken during the bubble growth process; they are not simulations or schematic representations.

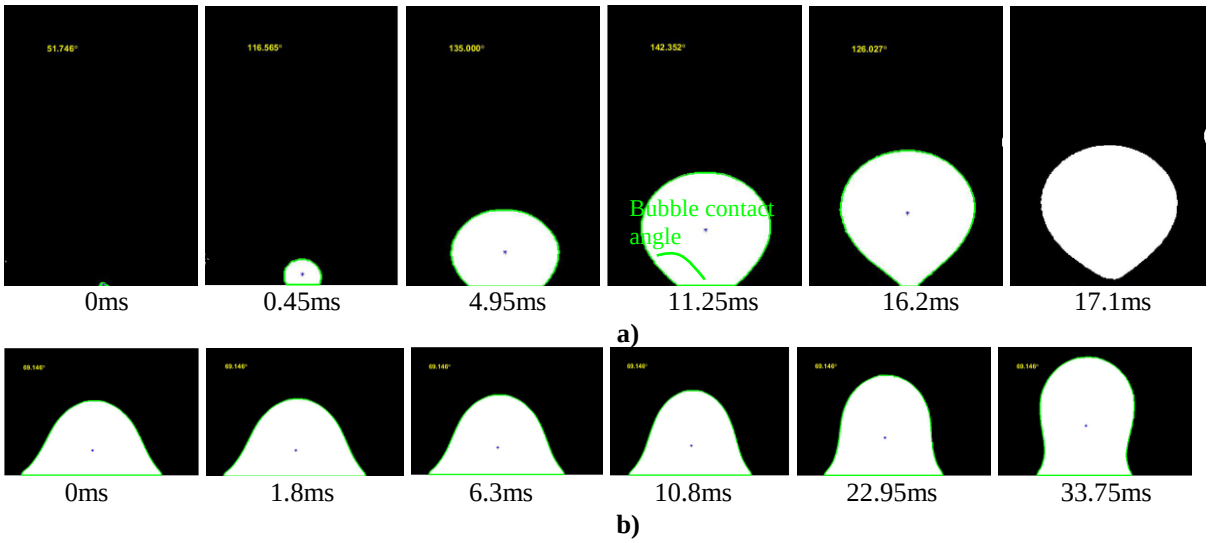

Figure 6. Temporal evolution of the bubble growth and detachment on: a) a hydrophilic surface, b) a superhydrophobic surface.

By comparison of the contact angles depicted in figure 5 with the schematic evolution shown in figure 6, it is not obvious that these angles approach the static or the quasi-static values at bubble formation and departure, as argued by Phan et al. (2010), but the bubble contact angle follows supplementary values to those of the micro-contact angle, which in turn and approximately (in average) close to the quasi-static angles. Hence, given this trend, one may perform a simple quantitative evaluation of this trend. Figure 7 depicts the bubble diameter as a function of the micro-contact angle, comparing the experimental results obtained here with those computed using the equation proposed in Phan et al. (2010):

$$D_b = \left(6\sqrt{\frac{3}{2}}\right)^{1/3} \left(\frac{\rho_l}{\rho_v}\right)^{-1/2} \left(\frac{\rho_l}{\rho_v} - 1\right)^{1/3} (\tan\theta)^{-1/6} L_c \tag{1}$$

in which $L_c = \sqrt{\frac{\sigma}{g(\rho_l - \rho_v)}}$ is the capillary length, which is representative of the bubble diameter.

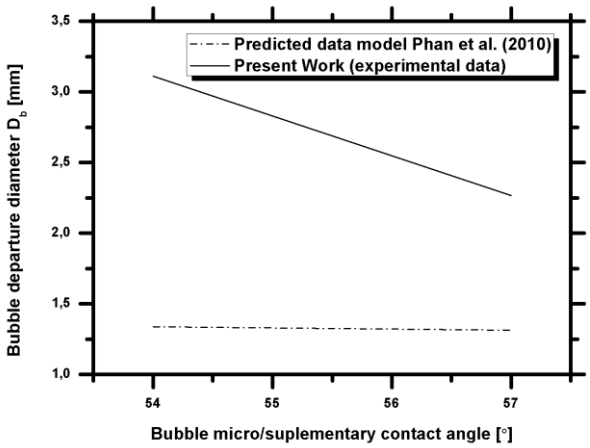

Figure 7. Bubble departure diameter as a function of the bubble micro-contact angle: comparison between the experimental results obtained in the present study and those provided by the expression proposed by Phan et al. (2010).

One can observe a general decreasing trend of the bubble diameter, as the micro-contact angle increases, which is followed by the experimental values and also by the predicted ones (although the later has a much smaller slope). However there is a significant disparity in terms of the values obtained for the bubble diameter. The main reason for this disparity is the fact that Phan et al. (2010) considers a single bubble nucleating from a single nucleation site. In the experimental conditions of the present work, the emerging bubble that was analyzed by the post-processing algorithm was most certainly the junction of a few very close and very small nucleation sites. They became activated at the same time due to microscopic thermal and mechanical interaction mechanisms, which resulted in a larger bubble emerging. One must note that even by having a bubble formed by various nucleation sites, the value for the contact angle becomes unchanged due to the fact that it only depends on fluid and surface properties and not the size of the bubble. Any satisfactory results are obtained for the superyhydrophobic surfaces or when the micro-contact angle is approached to the equilibrium and quasi-static angles. Although Phan et al. (2010) equation is only valid for contact angles lower than 90º, this analysis does not support such approach.

Further analyzing the bubble departure frequency, this is evaluated by Zuber's equation (Zuber, 1963), as a function of our experimental results obtained for the bubble diameter, as depicted in Figure 8.

The experimental results of the present work closely follow the trend predicted by Zuber(1963). However one must approach this result with caution as the experimental work only has three different bubble departure diameters for three different surfaces. This means that despite the fact that a general trend appears to be followed, deeper analysis must be performed. Nevertheless, these results suggest that the micro-contact angle provides a good quantification of the role of wettability on bubble dynamics, although there are several additional effects that must be considered, such as interaction mechanisms. Also, this analysis must be extended to explain the more complex processes occurring at superhydrophobic surfaces, for contact angles much larger than 90º.

Despite the particular description of the processes that is required to accurately predict the temporal evolution of bubble growth, qualitative analysis of Figures 4-6 suggest that in average, there may be a trend for the bubble and quasi-static angles to be supplemental, so that averaged quantities may follow trends with these angles. This is inferred in Figure 9, which considers the average bubble departure diameter (Figure 9a) and emission frequency (Figure 9b) as a function of bubble contact and micro-contact angles but also with the quasi-static angles.

The figure shows a clear trend of the bubble diameter to increase and consequently the frequency to decrease with the quasi-static and with the micro-contact angle, thus supporting some similarity between them and consequently supplementary evolution with the bubble contact angle. One must note that the results displayed in figure 9b) are obtained at high surface overheat for a more stable boiling process with fewer influence of interaction mechanisms that differ between wetting regimes. Results at lower surfaces overheat often have disparity in one or more points.

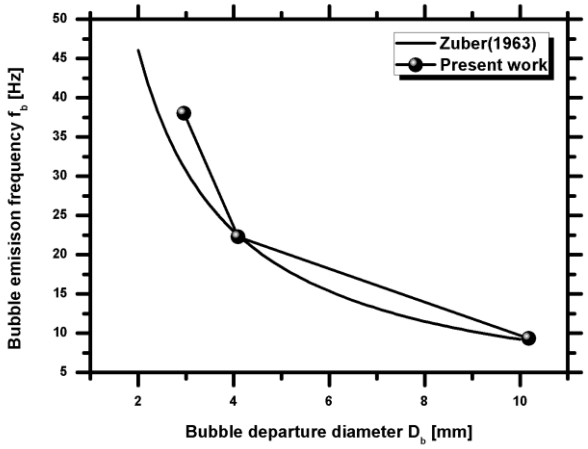

Figure 8. Bubble departure frequency provided by the expression proposed by Zuber (1963), as a function of the departure diameter (experimental results).

Taking advantage of the average quantities, evaluated to infer on possible trends between bubble departure diameter and frequency with the apparent contact angles, it is worth to perform an average analysis of bubble boiling for increasing steps of heat flux, as represented in Figure 10.

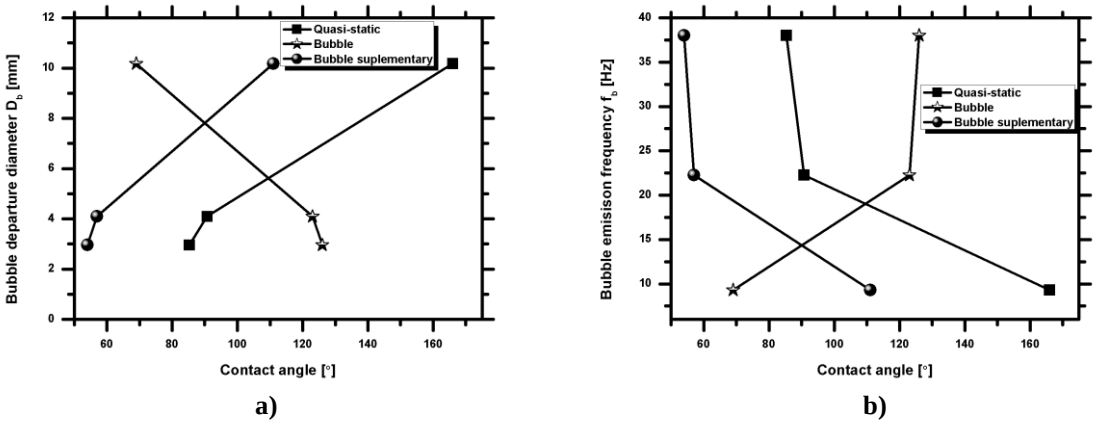

a) **b)**

Figure 9. Average a) bubble departure diameter and b) bubble departure frequency, as a function of the bubble contact angle, micro-contact angle and quasi-static angle.

The figure shows a clear trend of the bubble diameter to increase and consequently the frequency to decrease with the quasi-static and with the micro-contact angle, thus supporting some similarity between them and consequently supplementary evolution with the bubble contact angle. One must note that the results displayed in figure 9b) are obtained at high surface overheat for a more stable boiling process with fewer influence of interaction mechanisms that differ between wetting regimes. Results at lower surfaces overheat often have disparity in one or more points.

Taking advantage of the average quantities, evaluated to infer on possible trends between bubble departure diameter and frequency with the apparent contact angles, it is worth to perform an average analysis of bubble boiling for increasing steps of heat flux, as represented in Figure 10.

For the hydrophilic surfaces, the average bubble departure diameter slowly increases for gradually higher heat fluxes, as usually described in the literature (e.g., McHale and Garimella, 2010). The frequency follows the opposite trend, which in agreement with the most accepted expressions in the literature, as for instance that proposed by Zuber (1963), $f_b \propto (\sigma g(\rho_v-\rho_l)/\rho_l^2)^{1/4} . 1/D_b)$. Care must be nevertheless taken, when interpreting these average values, as they are affected by several other phenomena, which are not usually accounted in many of these expressions, such as bubble interaction and nucleation sites interaction. A different trend however is observed for the superhydrophobic surface. The bubble emission frequency is very slow (as the bubbles are very large) and so this increase is mainly due to bubble oscillations during the growth process, which seem to be more evident at higher heat fluxes and may promote the bubble detachment from the surface.

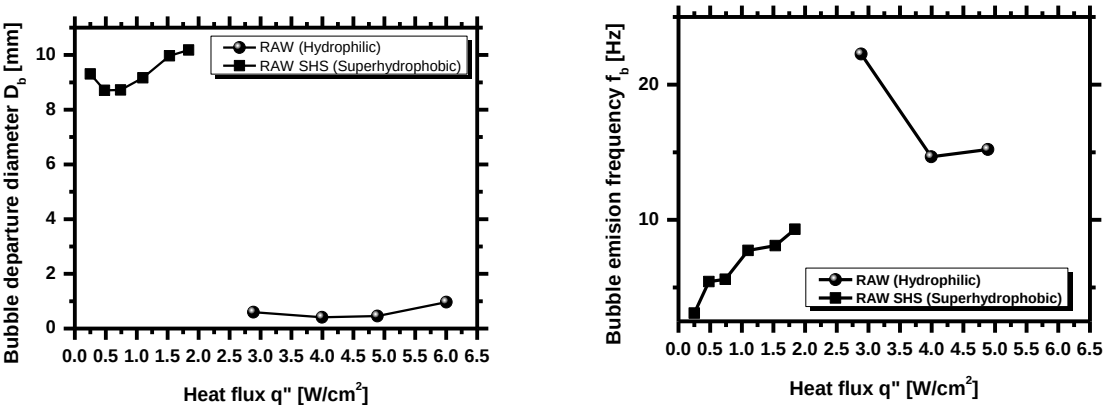

a) **b)**

Figure 10. a) Average bubble departure diameters and b) emission frequencies, as a function of the imposed heat flux.

NOMENCLATURE

q''	[W/cm^2]	Heat flux
D_b	[Hz]	Bubble departure diameter
C_p	[J/kgK]	Specific heat
f_b	[Hz]	Bubble emission frequency
h_{fq}	[kJ/kg]	Latent heat of evaporation
K	[W/(mK]	Thermal conductivity
L_c	[mm]	Characteristic length (capillary length)
R_a	[μm]	Surface mean roughness
R_z	[μm]	Surface peak-to-valley roughness
T	[ºC]	Temperature
Greek symbols		
$\Delta\theta$	[º]	Contact angles hysteresis
μ	[Ns/m^2]	Dynamic viscosity
θ_{adv}	[º]	Quasi-static advancing contact angle
θ_{rec}	[º]	Quasi-static receding contact angle
θ_{app}	[º]	Apparent equilibrium contact angle
ρ	[kg/m^3]	Density
σ	[N/m]	Liquid surface tension
Subscripts		
B		Bubble
L		Liquid
V		Vapor

FINAL REMARKS

The present study addresses the description of the heat transfer and bubble dynamics processes occurring for the boiling of water over surfaces with extreme wetting regimes, namely hydrophilicity and superhydrophobicity. The wettability is changed, mainly at the expense of modifying the surface chemistry. In agreement with the literature, the onset of boiling occurs at much lower surface superheat for the superhydrophobic surfaces. However, unlike observed for the boiling over hydrophilic surfaces, in this case the resulting boiling curve depicts a particular trend: the heat flux increases almost linearly with the superheat, until reaching a maximum value after which it does not further increase. Bubble dynamics may explain this progression: the system is at metastable equilibrium and the stochastic profile of the surface promotes the almost immediate coalescence of the bubbles so that a film vapor is almost immediately formed at 1ºC of superheating. Hence, a large bubble is formed over the entire surface, thus the heat transfer is reduced just after the onset of boiling. This behaviour is in agreement with the so-called "quasi-Leidenfrost" regime, recently reported in the literature.

Detailed analysis of bubble dynamics focuses on the temporal evolution of the bubble growth diameter together with bubble contact angle. This analysis shows substantial differences between the boiling over the hydrophilic vs the hydrophobic surfaces. Hence, besides the much slower departure frequency and larger bubble diameter of the bubbles generated on the superhydrophobic surface, the bubble contact angle does not vary much during the bubble growth process. As for the bubble growth over hydrophilic surfaces, the diameter increases with the bubble contact angle (i.e. decreases with the micro-angle) although the existing models cannot accurately predict the bubble growth diameter, as they do not account for interaction mechanisms either for the particular bubble growth phenomenon observed for the superhydrophobic surfaces.

The models and expressions currently existing in the literature can predict the trend of the bubble growth using the micro-contact angle (complementary to bubble contact angle), for hydrophilic surfaces, but cannot accurately predict bubble size, as they do not account for interaction mechanisms. Also they cannot describe the particular bubble growth phenomenon observed for the superhydrophobic surfaces. Quasi-static angles cannot provide any satisfactory results when used in the models to predict the bubble growth diameter, although they follow an evolution similar to that of the micro-contact angle and are supplemental to the bubble contact angle. In line with this, trends can be observed between the average bubble departure diameter and bubble departure frequency with both the bubble and the quasi-static advancing angle. These results suggest that the parameter which can accurately relate the bubble growth with the surface wettability is the bubble contact angle (or from the wall side, the so-called micro-contact angle), but apparent angles follow supplemental evolution, being therefore useful to identify qualitative trends.

ACKNOWLEDGEMENTS

The authors are grateful to Fundação para a Ciência e a Tecnologia (FCT) for partially financing the research under the framework of the project RECI/EMS-SIS/0147/2012 and for supporting T. Valente with a research fellowship. The authors also acknowledge FCT for supporting E. Teodori with a PhD fellowship (Ref.:SFRH/BD/88102/2012) and A.S. Moita with a Post-Doc Grant (Ref:SFRH/BPD/63788/2009).

REFERENCES

Abernethy, R.B., Benedict, R.P. and Dowdell, R.B., ASME measurements uncertainty, *J. Fluids Eng.*, Vol. 107, No. 2, pp. 161-164.

Antonini C., Amirfazli A. and Marengo M., 2012, Drop impact and wettability: from hydrophilic to superhydrophobic surfaces, *Phys. Fluids*, Vol. 24, 102104.

Betz, A.R., Jenkins, J., Kim, C.J. and Attinger, D., 2013, Boiling heat transfer on superhydrophobic, superhydrophilic, and superbiphilic surfaces, *Int. J. Heat Mass Transf.*, Vol. 57, pp. 733-741.

Bourdon, B., Di Marco, P., Rioboo, R., Marengo, M. and de Coninck, J., 2013, Enhancing the onset of pool boiling by wettability modification and nanometrically smooth surfaces, I*nt. Comm. Heat Mass Transf.*, Vol. 45, pp. 11-15.

Bourdon, B., Rioboo, R., Marengo, M., Gosselin, E. and de Coninck, J., 2012, Influence of the wettability on the boiling onset, *Langmuir*, Vol. 28, pp. 1618-1624.

Bushan, B. and Jung, Y.C., 2011, Natural and biomimetic artificial surfaces for hydrophobicity, self-cleaning, low adhesion and drag reduction, *Prog. Mat. Sci.*, Vol. 56, pp. 100-108.

Cheng, P., 1990, Automation of aisymmetric drop shape analysis using digital image processing, PhD Thesis, University of Toronto.

Corty, C. and Foust, A.S., 1955, Surface variables in nucleate boiling, *Chem. Eng. Prog. Symp. Ser.*, Vol. 57, No. 17, pp. 1-12.

Fritz, W., 1935, Maximum volume of vapour bubbles, Phys. Z, Vol. 36, pp. 379-384.

He, B., Patankar, A. and Lee, J., 2003, Multiple equilibrium droplet shapes and design criterions for rough hydrophobic surfaces, *Langmuir*, Vol. 19, pp. 4999-5003.

Malavasi, I., Bourdon, B., Di Marco, P., de Conink, J. And Marengo, M., 2015, Appearance of a low superheat "quasi-Leidenfrost" regime for boiling on superhydrophobic surfaces, Int. Comm. Heat Mass Transf., Vol. 63, pp. 1-7.

Matkovic, M. and Koncar, B., 2012, Bubble departure diameter prediction uncertainty, Science and Tech. Nuclear Inst., Vol. 2012, 7pp.

McHale, J.P. and Garimella, S.V., 2010, Bubble nucleation characteristics in pool boiling of a wetting liquid on smooth and rough surfaces, *Int. J. Multiphase Flow*, Vol. 36, pp. 249-260.

Moita, A.S., Teodori, E. and Moreira, A.L.N., 2015, Influence of surface topography in the boiling mechanisms, *Int. J. Heat Fluid Flow*, Vol. 52, pp. 50-63.

Mukherjee, A. and Kandlikar, S.G., 2007, Numerical study of single bubbles during nucleate pool boiling, *ASME J. Heat Transfer*, Vol. 126, pp. 1023-1039.

Phan, H.T., Caney, N., Marty, P., Colasson, S. and Gavillet, J., 2009, Surface wettability control by nanocoating: the effects on pool boiling heat transfer and nucleation mechanism, *Int. J. Heat Mass Transf.*, Vol. 53, pp. 5459-5471.

Phan, H.T., Caney, N., Marty, P., Colasson, S., Gavillet, J., 2010, A model to predict the effect of contact angle on the bubble departure diameter during heterogeneous boiling, Int. Comm. Heat Mass Transf., Vol. 37, pp. 964-969.

Rioboo, R., Marengo, M., Dall'Olio, S., Voué, M. and De Coninck, J., 2009, An Innovative Method to Control the Incipient Flow Boiling through Grafted Surfaces with Chemical Patterns, Langmuir, Vol. 25, Nº 11.

Takata, Y., Hidaka, S., Uraguchi, T. and Hu, L.W., 2006, Boiling feature on a super water-repellent surface, *Heat Transf. Eng.*, Vol. 27, pp. 25-30.

Teodori, E., Moita, A.S., Moreira, A.L.N., 2013, Characterization of pool boiling mechanisms over micro-patterned surfaces using PIV, Int. J. Heat Mass Transf., Vol. 66, pp. 261-270.

Valente, T., Teodori, E., Moita, A. S., Moreira, A. L. N., 2015, Effect of wettability on nucleate boiling, *Proc. 11th International Conference on Heat Transfer, Fluid Mechanics and Thermodynamics – HEFAT 2015*, Kruger National Park, South Africa, 20-23 July, pp. 168-177.

Zuber, N., 1963, Nucleate boiling: the region of isolated bubbles and the similarity with natural convection, Int. J. Heat Mass Transf., Vol. 6, pp. 53-78.